Quasielastic neutron scattering study of H motion in the hydrogen-stabilized C15-type phases

$HfTi_2H_x$ and $ZrTi_2H_x$

Quasielastic neutron scattering study of H motion in the hydrogen-stabilized C15-type phases HfTi₂Hₓ and ZrTi₂Hₓ

A V Skripov†, J Combet‡, H Grimm§, R Hempelmann‖ and V N Kozhanov†

† Institute of Metal Physics, Urals Branch of the Academy of Sciences, Ekaterinburg 620219, Russia
‡ Institut Laue–Langevin, F-38042 Grenoble, France
§ Institut für Festkörperforschung, Forschungszentrum Jülich, D-52425 Jülich, Germany
‖ Institut für Physikalische Chemie, Universität des Saarlandes, D-66041 Saarbrücken, Germany

Abstract. In order to clarify the mechanism of H diffusion in the hydrogen-stabilized phases HfTi$_2$H$_x$ and ZrTi$_2$H$_x$ with $x \approx 4$, we have performed high-resolution quasielastic neutron scattering measurements on HfTi$_2$H$_{3.5}$, HfTi$_2$H$_{4.0}$ and ZrTi$_2$H$_{3.9}$ over the temperature range 10–327 K. It is found that the diffusive motion of hydrogen in these systems can be described in terms of at least two frequency scales of H hopping. A small fraction of H atoms participates in the fast localized motion within the hexagons formed by interstitial g (Hf$_2$Ti$_2$ or Zr$_2$Ti$_2$) sites; this fraction increases with increasing temperature. The slower jump process corresponds to H motion on the nearly completely filled sublattice of interstitial e (HfTi$_3$ or ZrTi$_3$) sites; transitions from one e site to another imply a number of jumps over intermediate g sites. The parameters of H motion in HfTi$_2$H$_x$ and ZrTi$_2$H$_x$ are found to be close to each other. The temperature dependence of the characteristic rate τ_d^{-1} of the slower jump process in HfTi$_2$H$_4$ is well described by the Arrhenius law with the activation energy of 0.17 ± 0.02 eV.

1. Introduction

Hf–Ti and Zr–Ti alloys form only disordered solid solutions with the hexagonal close-packed (h.c.p.) lattice. However, it has been found that the absorption of hydrogen by disordered h.c.p. alloys ZrTi$_2$ and HfTi$_2$ results in the formation of the cubic phases ZrTi$_2$H$_x$ ($3 \leqslant x \leqslant 4$) [1] and HfTi$_2H_x$ ($3.5 \leqslant x \leqslant 4.5$) [2] with the ordered C15-type host lattice. In both systems the ordering of the host-metal lattice is induced by hydrogen; they return to the original disordered state when hydrogen is removed. Hydrogen atoms in C15-type Laves-phase hydrides AB$_2$H$_x$(AB$_2$D$_x$) are known to occupy two types of tetrahedral interstitial site: 32e (AB$_3$) and 96g (A$_2$B$_2$). In most of the C15 hydrides studied H (D) atoms occupy only g sites at low hydrogen concentrations; e sites start to be filled above $x \approx 3$ [3, 4]. Neutron diffraction measurements on the deuterium-stabilized C15-type HfTi$_2$D$_4$ [5] have shown that at room temperature about 3/4 of all D atoms occupy e sites, the rest of the D atoms being at g sites. In the related C15-type ZrTi$_2$D$_x$ phase, D atoms have been reported [1] to occupy only e sites. Note that the complete filling of the e-site sublattice corresponds to $x = 4$. Recent quasielastic neutron scattering (QENS) experiments [6–8] have clarified the mechanism of hydrogen diffusion in those C15-type compounds where H atoms occupy only g sites. In such systems the diffusive motion of hydrogen can be described in terms of two jump processes: the fast localized H motion within the hexagons formed by g sites and the slower hopping from one hexagon to another. However, little is known about the mechanisms of H motion in Laves

3313

phases with preferential e-site occupation. These mechanisms may be quite complex. In fact, the spatial arrangement of interstitial sites in the C15 lattice [4] suggests that a transition of an H atom from one e site to another occurs via at least two intermediate g sites. Nuclear magnetic resonance (NMR) measurements of the proton spin-relaxation rates in $ZrTi_2H_x$ ($x = 3.7$ and 3.9) [9] have revealed the coexistence of two frequency scales of H hopping. The faster frequency scale has been ascribed to a localized H motion, but the nature of this motion has not been elucidated. Hydrogen diffusion in $ZrTi_2H_x$ has also been studied by means of pulsed-field-gradient NMR for $x = 3.7$ [10] and QENS for $x = 3.6$ [11]. The results of these experiments appear to be consistent with H hopping on the sublattice of e sites. However, the faster frequency scale implying a possibility of localized H motion has not been investigated in references [10] and [11]. The aim of the present work is to clarify the microscopic picture of H hopping in the hydrogen-stabilized C15-type phases $HfTi_2H_x$ and $ZrTi_2H_x$ with preferential e-site occupation. We have performed high-resolution QENS measurements for $HfTi_2H_{3.5}$, $HfTi_2H_{4.0}$ and $ZrTi_2H_{3.9}$ over the temperature range 10–327 K. The emphasis is placed on the properties of the new hydrogen-stabilized $HfTi_2H_x$ system [2]; for comparison, QENS spectra of $ZrTi_2H_{3.9}$ have been recorded at a number of temperatures. Our measurements have confirmed the existence of a fast localized H motion in both $HfTi_2H_x$ and $ZrTi_2H_x$.

2. Experimental details

The preparation of $HfTi_2H_x$ ($x = 3.5$ and 4.0) and $ZrTi_2H_{3.9}$ samples was analogous to that described in [2, 9]. X-ray diffraction analysis has shown that all these samples are single-phase compounds with C15-type host-lattice structure and the lattice parameters $a_0 = 8.10$ Å ($HfTi_2H_{3.5}$), 8.09 Å ($HfTi_2H_4$) and 8.18 Å ($ZrTi_2H_{3.9}$). QENS measurements were performed on the high-resolution backscattering spectrometers IN10 (Institut Laue–Langevin, Grenoble) and BSS1 (Forschungszentrum Jülich). Both spectrometers use the Si(111) monochromator and analysers selecting the neutron wavelength $\lambda = 6.271$ Å. The ranges of energy transfer $\hbar\omega$ in our experiments were ± 13.6 μeV (IN10) and ± 15.5 μeV (BSS1), the energy resolution FWHM being 0.9 and 1.2 μeV, respectively. The ranges of momentum transfer $\hbar Q$ studied corresponded to Q-ranges of 0.41–1.94 Å^{-1} (IN10) and 0.16–1.88 Å^{-1} (BSS1). The powdered samples were placed into flat Al containers with depths of 0.3 mm ($HfTi_2H_x$) and 0.56 mm ($ZrTi_2H_{3.9}$). The planes of the containers were oriented along the directions $2\theta \approx 84°$ ($HfTi_2H_x$) and $2\theta \approx 83°$ ($ZrTi_2H_{3.9}$) corresponding to (111) Bragg reflections for the samples. For $HfTi_2H_x$ the QENS spectra were recorded using IN10 at the temperatures 10, 170, 195, 210, 225, 239, 289, 299, 310 and 325 K for $x = 4$ and at 10, 224, 299 and 325 K for $x = 3.5$. The $ZrTi_2H_{3.9}$ sample was studied on BSS1 at the temperatures 12, 180, 201, 223, 303 and 327 K. The raw experimental data were corrected for absorption and self-shielding using the standard ILL programs and for the background scattering using the measured spectra of the empty sample containers in the cryostat. The instrumental resolution functions were determined from the QENS spectra of $HfTi_2H_x$ at 10 K (IN10) and from the QENS spectra of vanadium plate at room temperature (BSS1).

3. Results and discussion

3.1. QENS spectra: an overview

The experimental QENS spectra for $HfTi_2H_{3.5}$, $HfTi_2H_4$ and $ZrTi_2H_{3.9}$ show qualitatively similar behaviour over the temperature range studied. Between 170 and 239 K the spectra can be satisfactorily described by a sum of two components: a narrow 'elastic' line represented by

the spectrometer resolution function $R(Q, \omega)$ and a resolution-broadened Lorentzian 'quasi-elastic' line. As an example of the data, figure 1 shows the QENS spectrum of $HfTi_2H_4$ recorded at 225 K for $Q = 1.94$ Å^{-1}. As the first step of the analysis, we have fitted the experimental spectra with the model incoherent scattering function

$$S_{inc}(Q, \omega) = A_0(Q)\delta(\omega) + [1 - A_0(Q)]L(\omega, \Gamma) \tag{1}$$

convoluted with $R(Q, \omega)$. Here $\delta(\omega)$ is the 'elastic' δ-function, $L(\omega, \Gamma)$ is the 'quasielastic' Lorentzian with the half-width Γ and $A_0(Q)$ is the elastic incoherent structure factor (EISF). The relative intensity of the 'quasielastic' component is found to increase with increasing Q, its half-width Γ being nearly Q-independent. These features are typical of the case of spatially confined (localized) motion [12]. The value of Γ is proportional to the hydrogen hopping rate τ_l^{-1}, and $A_0(Q)$ contains information on the geometry of the localized motion [12]. Thus, our results are consistent with the existence of a localized H motion for $HfTi_2H_{3.5}$, $HfTi_2H_4$ and $ZrTi_2H_{3.9}$ with the characteristic hopping rates being within the frequency 'window' of the backscattering spectrometers ($\sim 3 \times 10^8$ to 3×10^9 s^{-1}) for 170 K $\leqslant T \leqslant$ 239 K. Above 289 K the effects of the long-range H diffusion become observable. In this temperature range the hopping rate of the localized H motion is higher than the frequency 'window' of the backscattering spectrometers; therefore, instead of the low-temperature 'quasielastic' line we observe a flat background. As expected, this background is Q-dependent, increasing with increasing Q. On the other hand, the low-temperature 'elastic' line shows a pronounced broadening above 289 K. In this range the QENS spectra can be reasonably described by a
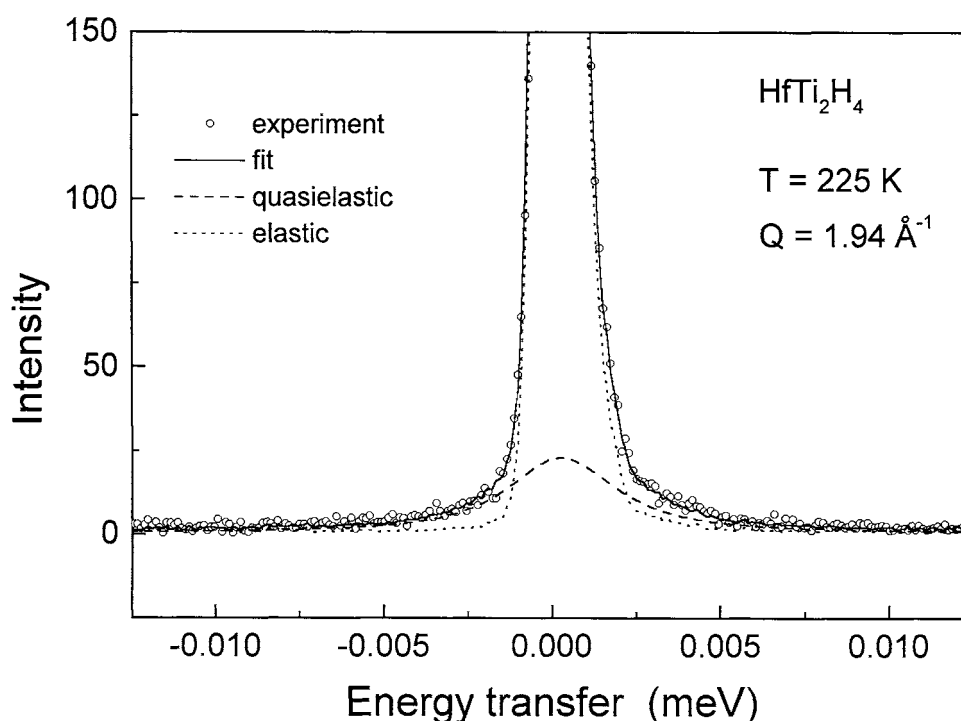

Figure 1. The quasielastic neutron scattering spectrum for $HfTi_2H_4$ measured on IN10 at 225 K and $Q = 1.94$ Å^{-1}. The solid line shows the fit of the two-component model to the data. The dotted line represents the spectrometer resolution function ('elastic' component), and the dashed line shows the Lorentzian 'quasielastic' component.

sum of a flat background and a single Lorentzian convoluted with the instrumental resolution function. The observed Q-dependence of the half-width Γ_0 of this Lorentzian is typical for the case of jump diffusion [12]. For parametrization of the $\Gamma_0(Q)$ dependence we have used the orientationally averaged Chudley–Elliott model [13] describing the diffusion with the constant jump length L and with random distribution of jump directions. The values of Γ_0 are found to increase with increasing temperature. Thus, using the backscattering neutron spectrometers in different temperature ranges, we have probed both the localized H motion and the long-range H diffusion in the hydrogen-stabilized phases $HfTi_2H_x$ and $ZrTi_2H_x$. In the following sections we shall discuss the parameters of these two types of H motion.

3.2. Localized hydrogen motion

As noted above, in the temperature range 170–239 K the observed QENS spectra for $HfTi_2H_x$ and $ZrTi_2H_{3.9}$ can be satisfactorily described in terms of equation (1) with a nearly Q-independent half-width Γ. In order to assess Γ and $A_0(Q)$ at each temperature, we have used a simultaneous fit of $S_{inc}(Q, \omega)$ to the data at all Q with a common value of Γ. The temperature dependence of the fitted quasielastic half-width Γ for $HfTi_2H_x$ and $ZrTi_2H_{3.9}$ is shown in figure 2. It can be seen that the half-width increases with increasing temperature, the values of Γ for $HfTi_2H_x$ being somewhat higher than the corresponding values for $ZrTi_2H_{3.9}$. Figure 3 shows the behaviour of the elastic incoherent structure factor $A_0(Q)$ for $HfTi_2H_4$ at $T = 195$ and 225 K. A similar shape of the Q-dependence of the EISF is observed for $HfTi_2H_{3.5}$ and $ZrTi_2H_{3.9}$. The measured EISF appears to be temperature dependent, decreasing with increasing T. This feature has also been found for the EISF for TaV_2H_x [6], $ZrCr_2H_x$ [7] and $ZrMo_2H_x$ [8]. In order to account for the temperature dependence of the measured EISF, we have to assume that only a fraction p of H atoms participates in the fast localized motion, and this fraction increases with temperature. The fraction $1 - p$ of 'static' protons (on the frequency scale determined by the spectrometer resolution) contributes only to the 'elastic' line and makes the observed values of $A_0(Q)$ higher than those expected in the case of $p = 1$. We shall return to the discussion of this feature below. In order to elucidate the geometry of the
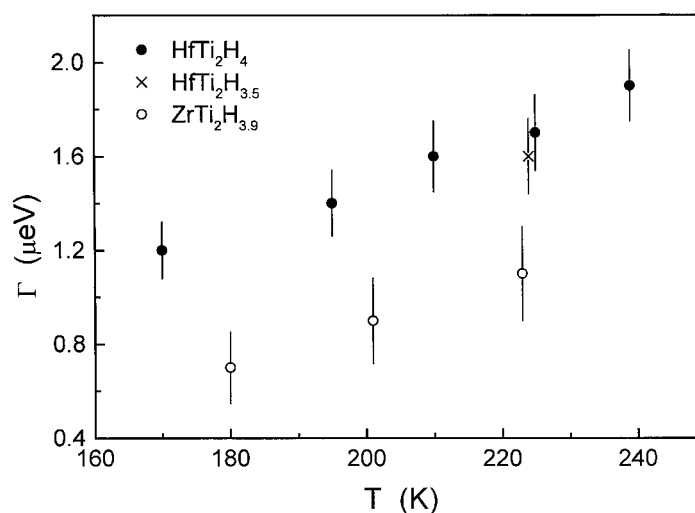

Figure 2. The temperature dependence of the half-width (HWHM) of the 'quasielastic' line for $HfTi_2H_4$, $HfTi_2H_{3.5}$ and $ZrTi_2H_{3.9}$.
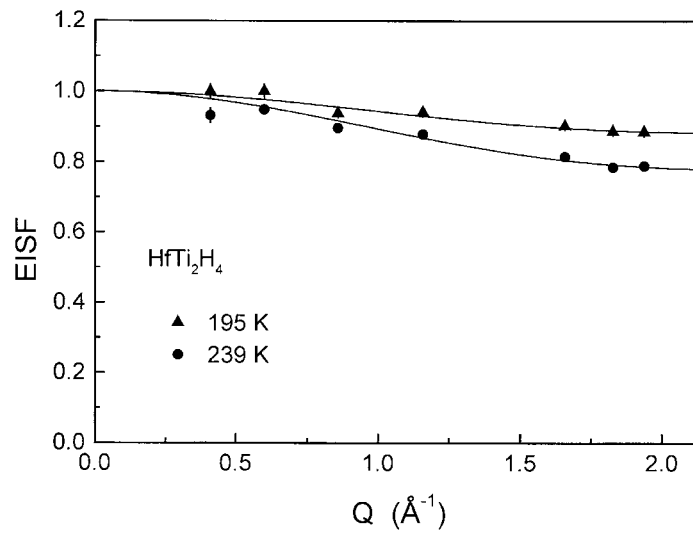
Figure 3. The elastic incoherent structure factor for $HfTi_2H_4$ as a function of Q at $T = 195$ K and 239 K. The solid lines represent the fits of the six-site model (equation (5)) with the fixed $r = 1.25$ Å to the data.

localized motion, we have to consider the spatial arrangement of the interstitial sites occupied by hydrogen. The network of e and g sites is shown schematically in figure 4. It is often assumed [10, 11] that e sites in the C15 lattice form a face-centred cubic (f.c.c.) sublattice with the lattice parameter $a_0/2$. However, this is true only if the positional parameter X_e of hydrogen
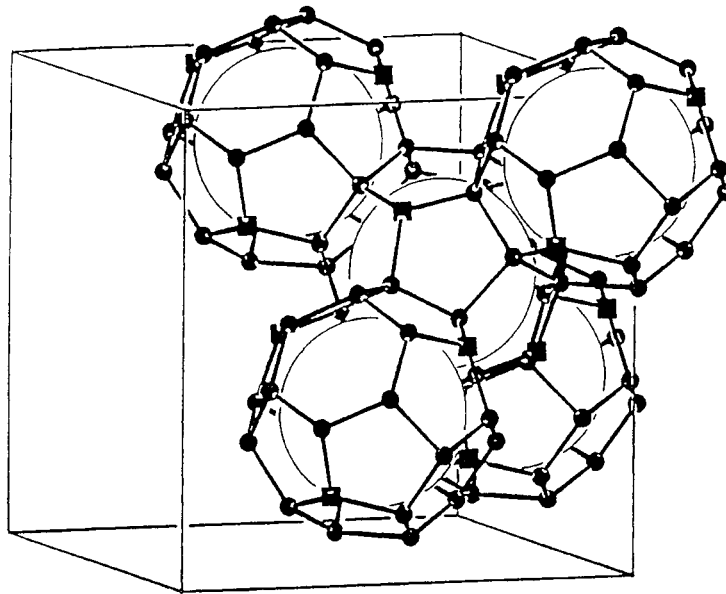

Figure 4. The spatial arrangement of interstitial sites in C15-type AB_2 compound (from [14]). Full squares: e sites; full circles: g sites; large open circles: A atoms.

at e sites is equal to 0.25. The values of X_e determined from neutron diffraction experiments on C15-type deuterides are usually higher than 0.25 [4]. In particular, for HfTi$_2$D$_4$ and ZrTi$_2$D$_4$ the experimental X_e-values are 0.267 [5] and 0.262 [1], respectively. This means that hydrogen atoms occupying e sites are displaced from their positions in the ideal f.c.c. sublattice. Such displacements change the distances between the nearest e sites in the following way: instead of 12 nearest-neighbour sites at the distance $a_0/2\sqrt{2} \approx 0.354a_0$ in the f.c.c. sublattice, each e site has three neighbours at the distance r_{e1}, six neighbours at r_{e2} and three neighbours at r_{e3}, $r_{e1} < r_{e2} < r_{e3}$. The values of r_{e1}, r_{e2} and r_{e3} depend on X_e. Using the experimental X_e-value for HfTi$_2$D$_4$ we obtain $r_{e1} = 0.305a_0$, $r_{e2} = 0.355a_0$ and $r_{e3} = 0.402a_0$. It is interesting to note that e sites separated by r_{e1} form tetrahedra. In other words, the e-site sublattice is split into tetrahedra, the distance between the sites within tetrahedra (r_{e1}) being shorter than the shortest distance between the sites belonging to different tetrahedra (r_{e2}). Therefore, in principle, the structure of the e-site sublattice is compatible with the possibility of localized H motion. The sublattice of g sites consists of hexagons (figure 4), the distance r_{g1} between the nearest sites within the hexagon being shorter than the distance r_{g2} between the nearest sites on different hexagons. This structure is favourable for the occurrence of localized H motion. In fact, the fast localized motion of hydrogen atoms within g-site hexagons has been observed in a number of C15-type compounds [6–8]. The values of r_{g1} and r_{g2} depend on the positional parameters of hydrogen atoms at g sites, X_g and Z_g. Using the experimental positional parameters of D atoms at g sites in HfTi$_2$D$_4$ ($X_g = 0.063$, $Z_g = 0.892$ at 200 K) [5], we obtain $r_{g1} = 0.155a_0$, $r_{g2} = 0.175a_0$. Note that the g–g distances r_{g1} and r_{g2} are nearly two times shorter than the corresponding e–e distances r_{e1} and r_{e2}. Thus, the structures of both e-site and g-site sublattices in the C15 lattice are compatible with the possibility of localized hydrogen motion, implying H hopping within tetrahedra (e sites) or within hexagons (g sites). An additional possible mechanism of the localized H motion corresponds to back-and-forth jumps within e–g pairs. For HfTi$_2$H$_x$ the nearest-neighbour e and g sites are separated by $r_{eg} = 0.172a_0$. Let us check now whether these types of H motion are consistent with the observed Q-dependence of the EISF. For the jumps within e–g pairs we may use the standard two-site model expression for $A_0(Q)$ [12]. Taking into account that only a fraction $p(T)$ of H atoms participates in the localized motion, it can be shown that for the two-site model the incoherent scattering function is given by equation (1) with

$$A_0(Q, T) = 1 - p(T) + \frac{1}{2}p(T)[1 + j_0(Qd)] \tag{2}$$

where $j_0(x)$ is the spherical Bessel function of zeroth order and d is the distance between two sites. The fit of equation (2) to the $A_0(Q)$ data for HfTi$_2$H$_4$ at 225 K results in $p = 0.25 \pm 0.01$, $d = 2.12 \pm 0.11$ Å. The fitted value of d is considerably higher than the distance between the nearest-neighbour e and g sites, $r_{eg} = 0.172a_0 \approx 1.39$ Å. This means that the observed Q-dependence of the EISF does not support the model of jumps within e–g pairs. Using the approach described in references [12], we have found that for a model of jumps between four sites forming a tetrahedron with the edge R, the incoherent scattering function is given by equation (1) with

$$A_0(Q) = \frac{1}{4}[1 + 3j_0(QR)]. \tag{3}$$

In the case where $p \neq 1$, we obtain

$$A_0(Q, T) = 1 - p(T) + \frac{1}{4}p(T)[1 + 3j_0(QR)]. \tag{4}$$

The fit of equation (4) to the $A_0(Q)$ data for HfTi$_2$H$_4$ at 225 K yields $p = 0.164 \pm 0.007$, $R = 2.11 \pm 0.11$ Å. The fitted value of R appears to be smaller than the shortest e–e distance

$r_{e1} = 0.305a_0 = 2.47$ Å. Considering the possibility of localized H motion on g-site hexagons, we can use the expression for the EISF obtained for the model of hopping between six equally spaced sites on a circle of radius r [12]. In the case where $p \neq 1$, this expression has the form

$$A_0(Q, T) = 1 - p(T) + \frac{1}{6}p(T)[1 + 2j_0(Qr) + 2j_0(Qr\sqrt{3}) + j_0(2Qr)]. \quad (5)$$

The fit of equation (5) to the $A_0(Q)$ data for $HfTi_2H_4$ at 225 K yields $p = 0.174 \pm 0.008$, $r = 1.27 \pm 0.07$ Å. Note that the fitted value of r is very close to the value $r = r_{g1} = 0.155a_0 = 1.25$ Å resulting from the structure. Thus, the analysis of the Q-dependence of the EISF shows that for the model of localized H motion on g-site hexagons the fit parameters are consistent with the structure of the g-site sublattice. Although the model of localized H motion on e-site tetrahedra can also describe the observed Q-dependence of the EISF, the fitted value of the jump length differs from the shortest e–e distance. There are also some additional arguments against the possibility of localized H motion on the e-site sublattice.

(1) The spatial arrangement of g and e sites in the C15 lattice (see figure 4) does not support the idea of direct e–e jumps. As can be seen from this figure, a transition from one e site to another is likely to occur via two intermediate g sites. Each e site has three nearest-neighbour g sites at the distance $r_{eg} = 0.172a_0 \approx 1.39$ Å. Note that r_{eg} is considerably shorter than r_{e1}, being nearly equal to r_{g2}.

(2) The sublattice of e sites in $HfTi_2H_4$ is close to being completely filled; this is expected to suppress a localized H motion on e sites.

(3) The observed localized H motion is quite fast even at low temperatures.

In fact, NMR measurements of the proton spin–lattice relaxation rate T_1^{-1} in $HfTi_2H_4$ [15] have revealed a strong motional contribution to T_1^{-1} down to $T \approx 90$ K. This indicates the presence of H motion with the hopping rate of the order of 10^6 s^{-1} or higher at 90 K. Since the hydrogen hopping rate in Laves phases is found to decrease strongly with increasing intersite distance [7, 8], such a fast H motion can hardly be reconciled with the shortest e–e distance $r_{e1} \approx 2.47$ Å. On the basis of these considerations we can conclude that the observed localized H motion in the hydrogen-stabilized $HfTi_2H_x$ phase implies H jumps within g-site hexagons. While most of the H atoms reside at e sites, the rest of them are located on the g-site sublattice, where they can participate in the localized motion. According to recent neutron diffraction measurements on $HfTi_2D_4$ [5], the fraction n_g of hydrogen atoms occupying g sites increases with increasing temperature. Similar considerations are also applicable to the related hydrogen-stabilized $ZrTi_2H_x$ phase. Although hydrogen atoms have been reported to occupy only e sites in $ZrTi_2D_4$ [1], the treatment of the neutron diffraction data in [1] was semi-quantitative (the diffraction profile was not refined), and therefore a small g-site occupancy cannot be excluded. Moreover, recent x-ray diffraction studies of the phase diagrams of $HfTi_2$–H and $ZrTi_2$–H systems over wide ranges of hydrogen contents [16] have shown that for the hydrogen-stabilized C15-type phases $HfTi_2H_x$ and $ZrTi_2H_x$ a single-phase state at room temperature is retained up to $x = 4.5$ and 4.7, respectively. Since the complete filling of the e-site sublattice corresponds to $x = 4$, these results indicate that g sites should also be partially occupied by hydrogen in $ZrTi_2H_x$. By fixing r in equation (5) to the value $r_{g1} = 1.25$ Å, resulting from the structure, we have found reasonable fits of the six-site model to the $A_0(Q)$ data for $HfTi_2H_x$ at all temperatures in the range 170–239 K with p as the only fit parameter. The results of these fits are shown as solid curves in figure 3. A similar approach has been used for $ZrTi_2H_{3.9}$, the value of r being fixed to $r_{g1} = 1.27$ Å. The temperature dependence of p resulting from these fits is shown in figure 5. It can be seen that for both systems the value of p increases with increasing temperature. This is consistent with the observed temperature dependence of the fraction of hydrogen atoms occupying g sites, n_g, in $HfTi_2D_4$ [5]. Although
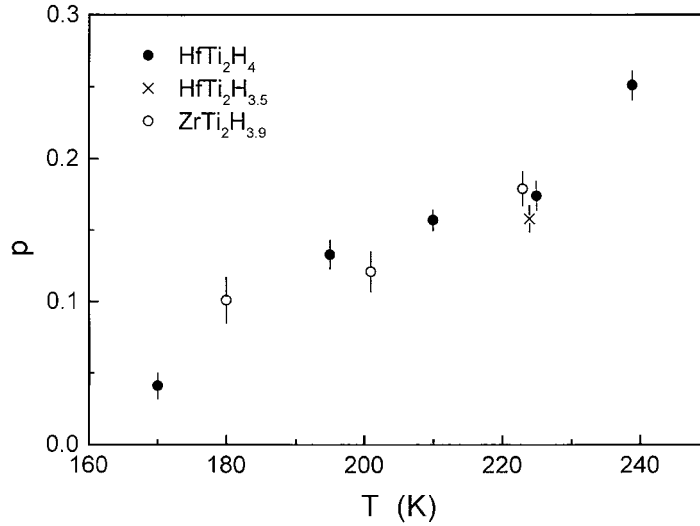
Figure 5. The temperature dependence of the fraction of protons participating in the fast localized motion, as determined from the fits of the six-site model to the data for $HfTi_2H_4$, $HfTi_2H_{3.5}$ and $ZrTi_2H_{3.9}$.

the values of p and n_g (which may also depend on hydrogen isotope) are not expected to be the same, they are likely to be of the same order of magnitude. According to [5], the n_g-value for $HfTi_2D_4$ at 200 K is 0.196; this is close to the value $p = 0.133$ obtained from the $A_0(Q)$ fit for $HfTi_2H_4$ at 195 K. A more rigorous approach to the data analysis should imply a simultaneous fit of $S_{inc}(Q, \omega)$ for the six-site model with the fixed $r = 1.25$ Å or 1.27 Å to the spectra at all Q. Taking into account that only a fraction p of protons participates in the fast localized motion, $S_{inc}(Q, \omega)$ for the six-site model [12] can be written in the form

$$S_{inc}(Q, \omega) = A_0(Q)\delta(\omega) + p \sum_{i=1}^{3} A_i(Q)L(\omega, \Gamma_i) \tag{6}$$

where $A_0(Q)$ is given by equation (5), $L(\omega, \Gamma_i)$ is the Lorentzian function with the half-width Γ_i, $\Gamma_1 = 0.5\tau_l^{-1}$, $\Gamma_2 = 1.5\tau_l^{-1}$, $\Gamma_3 = 2\tau_l^{-1}$ and τ_l is the mean time between two successive jumps of a proton within a hexagon. Thus, for the six-site model the quasielastic line is expected to consist of three Lorentzian components with different half-widths Γ_i and Q-dependent amplitudes $A_i(Q)$. However, as has been noted previously [17], because of the limited experimental accuracy it is difficult to distinguish between such a three-component quasielastic line and a single Lorentzian with a Q-independent width in the case of a rather weak quasielastic line coexisting with a strong elastic one. In fact, we have found that the quality of simultaneous fits based on equation (6) with the fit parameters τ_l^{-1} and p is comparable to the quality of simultaneous fits based on equations (1) and (5) with a common Γ. Moreover, the values of p obtained from these two types of fit are nearly the same, and the common Γ value appears to be close to $0.6\tau_l^{-1}$.

3.3. Long-range diffusion of hydrogen

As noted in section 3.1, above 289 K the experimental QENS spectra for $HfTi_2H_x$ and $ZrTi_2H_{3.9}$ can be satisfactorily described by a sum of a flat background and a single Lorentzian convoluted with the instrumental resolution function. The Q-dependence of the half-width Γ_0 of

this Lorentzian is typical of the case of jump diffusion [12]. The low-Q range (corresponding to $QL \ll 1$) has been studied only for $ZrTi_2H_{3.9}$ in the measurements on BSS1. However, at the temperatures of our measurements (303 K and 327 K) the line broadening at low Q is too small to be reliably determined with the available instrumental resolution. Examples of the dependence $\Gamma_0(Q)$ over the entire Q-range studied are shown in figure 6. For parametrization of this dependence we have used the orientationally averaged Chudley–Elliott model [13]. The corresponding form of $\Gamma_0(Q)$ is

$$\Gamma_0(Q) = \frac{\hbar}{\tau_d} \left(1 - \frac{\sin QL}{QL} \right) \tag{7}$$

where τ_d is the mean time between two successive H jumps leading to long-range diffusion. The fits of equation (7) to the data are shown by the solid lines in figure 6. The temperature dependences of τ_d^{-1} resulting from the Chudley–Elliott fits are presented in figure 7. As can be seen from this figure, for $HfTi_2H_4$ the behaviour of τ_d^{-1} is satisfactorily described by the Arrhenius law:

$$\tau_d^{-1} = \tau_{d0}^{-1} \exp(-E_a^\tau/k_B T). \tag{8}$$

For $HfTi_2H_4$ the activation energy E_a^τ derived from the Arrhenius fit is 0.17 ± 0.02 eV, and the pre-exponential factor τ_{d0}^{-1} is $(4.6 \pm 1.5) \times 10^{11}$ s^{-1}. The values of τ_d^{-1} for $ZrTi_2H_{3.9}$ are somewhat higher than the corresponding values for $HfTi_2H_x$ samples. Fernandez *et al* [11] have found from their QENS data for $ZrTi_2H_{3.6}$ that $E_a^\tau = 0.19 \pm 0.01$ eV and $\tau_{d0}^{-1} = (6.7 \pm 1.8) \times 10^{11}$ s^{-1}. Thus, our results for E_a^τ and τ_{d0}^{-1} for $HfTi_2H_4$ are close to the corresponding results [11] for $ZrTi_2H_{3.6}$. The values of the effective jump length L resulting from the Chudley–Elliott fits for $HfTi_2H_4$, $HfTi_2H_{3.5}$ and $ZrTi_2H_{3.9}$ appear to be close to each other. For example, the fitted values of L are 2.75 ± 0.03 Å for $HfTi_2H_4$ at 322 K, 2.78 ± 0.03 Å for $HfTi_2H_{3.5}$ at 322 K and 2.74 ± 0.08 Å for $ZrTi_2H_{3.9}$ at 327 K. These values can be compared to the previous estimates of L for $ZrTi_2H_x$: 2.8 ± 0.4 Å from the Chudley–Elliott fits to the
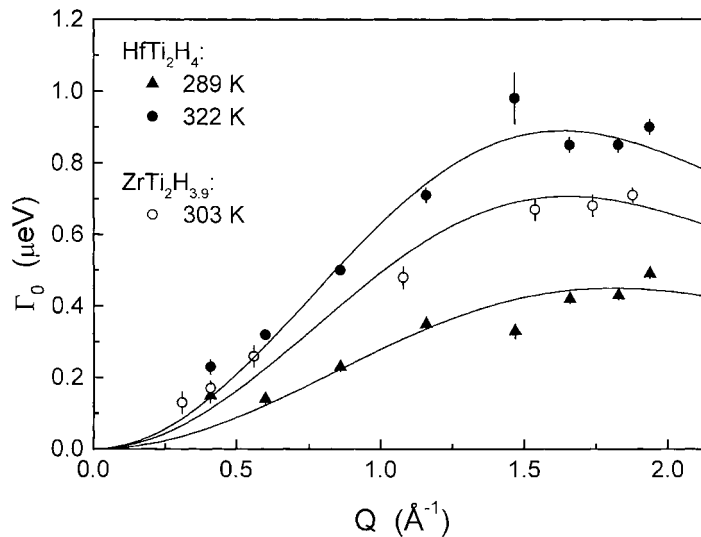

Figure 6. The half-width of the narrow Lorentzian QENS component as a function of Q for $HfTi_2H_4$ at $T = 289$ and 322 K and for $ZrTi_2H_{3.9}$ at $T = 303$ K. The solid lines show the fits of the Chudley–Elliott model (equation (7)) to the data.

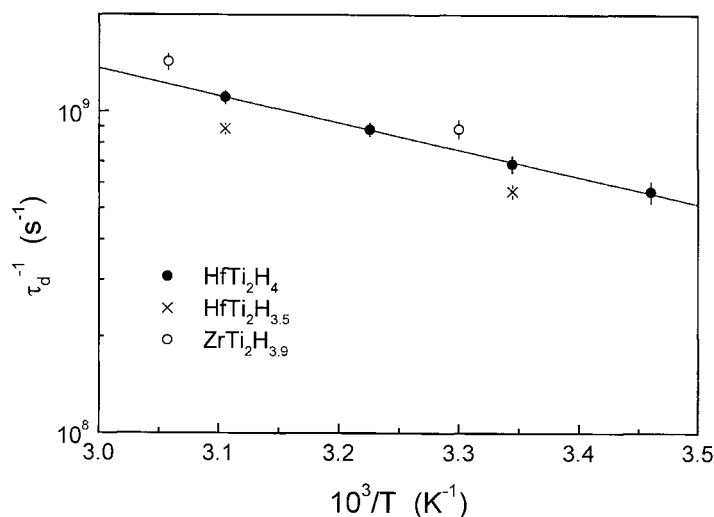**Figure 7.** The temperature dependence of the hydrogen hopping rate τ_d^{-1} derived from the Chudley–Elliott fits (equation (7)). The solid line shows the Arrhenius fit to the data for $HfTi_2H_4$.

QENS data for $ZrTi_2H_{3.6}$ [11] and 2.5 ± 0.2 Å from the proton T_1^{-1} and PFG-NMR data for $ZrTi_2H_{3.7}$ [10]. Note that these values are considerably larger than the nearest-neighbour g–g distances r_{g1} (1.25 Å for $HfTi_2H_4$ and 1.27 Å for $ZrTi_2H_{3.9}$) and the nearest-neighbour e–g distances r_{eg} (1.39 Å for $HfTi_2H_4$ and 1.41 Å for $ZrTi_2H_{3.9}$). On the other hand, the fitted values of L lie between the nearest-neighbour e–e distances r_{e1} and r_{e2} (2.47 and 2.87 Å for $HfTi_2H_4$ and 2.49 and 2.90 Å for $ZrTi_2H_{3.9}$). However, this fact can hardly be interpreted as evidence that the direct e–e jumps of H atoms form the main diffusion path. Indeed, for the model implying two timescales of H motion the slower timescale τ_d may not coincide with the mean residence time of a hydrogen atom at an interstitial site. For the motion of H atoms on the g-site sublattice the value of τ_d is determined by the mean residence time of a hydrogen atom at a g-site hexagon [6, 7]. In the case of the nearly completely filled e-site sublattice and the nearly empty g-site sublattice, a hydrogen atom participating in the long-range diffusion is expected to jump out of the e-site sublattice and to perform a number of jumps on the g-site sublattice before it finds a vacant e site. A similar mechanism of H diffusion has been reported for the ordered β-V_2H phase [18], where the filled (110) planes of octahedral interstitial sites are separated by the empty (110) planes. For this jump model τ_d is determined essentially by the average time spent by a hydrogen atom on the g-site sublattice before it finds a vacant e site, and L is the measure of the displacement for the period τ_d. The fitted value of L for $HfTi_2H_4$ is found to increase with increasing temperature; it changes from 2.48 ± 0.05 Å at 289 K to 2.75 ± 0.03 Å at 322 K. This may be related to the increase in g-site occupancy [5] with increasing T. The relation between the tracer diffusion coefficient D and the values of τ_d and L is given by

$$D = \frac{L^2}{6\tau_d}. \tag{9}$$

We assume here that the tracer correlation factor [19] for H diffusion is equal to 1. This assumption may seem questionable, since the H concentration in our samples is not low. However, if the main diffusion path includes jumps on the nearly empty g-site sublattice, such an assumption may be justified. Using the values of τ_d and L derived from the Chudley–Elliott

fits, we can obtain D from equation (9). The resulting D-values are shown in figure 8. At room temperature the D-value for $ZrTi_2H_{3.9}$ is about a factor of 2 higher than that obtained from the PFG-NMR measurements [10] for $ZrTi_2H_{3.7}$. In the temperature range 289–322 K the behaviour of D for $HfTi_2H_4$ is well described by the Arrhenius law with the activation energy $E_a^D = 0.23 \pm 0.01$ eV and the pre-exponential factor $D_0 = (4.6 \pm 1.6) \times 10^{-4}$ cm^2 s^{-1}. Note that the activation energy E_a^D describing the temperature dependence of the tracer diffusion coefficient is higher than the activation energy E_a^τ for τ_d^{-1}. A similar feature has been found for C15-type $ZrCr_2H_{0.45}$ [7] over a considerably wider temperature range. The difference between E_a^D and E_a^τ results from the observed temperature dependence of L. Since L is found to increase with increasing temperature, it follows from equation (9) that D grows with temperature faster than τ_d^{-1}. The value of E_a^D for $HfTi_2H_4$ appears to be close to the corresponding value obtained from the model-independent PFG-NMR measurements of H diffusivity in $ZrTi_2H_{3.7}$ (0.21 ± 0.01 eV) [10].
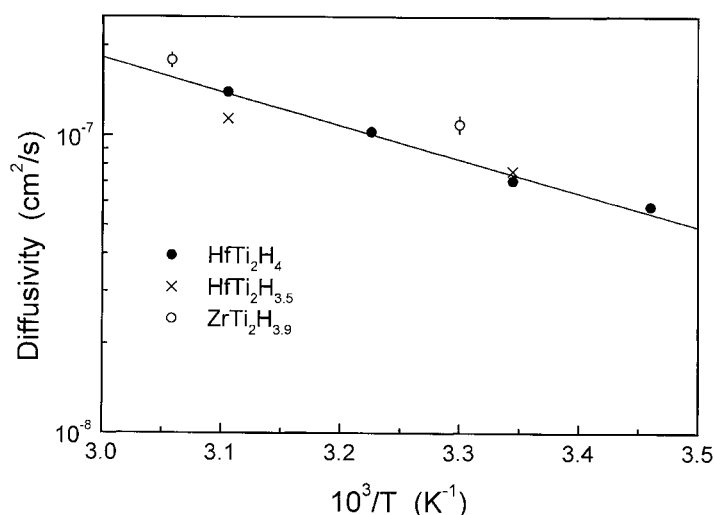

Figure 8. The temperature dependence of the tracer diffusion coefficient of hydrogen determined from the Chudley–Elliott fits (equations (7) and (9)). The solid line shows the Arrhenius fit to the data for $HfTi_2H_4$.

4. Conclusions

Quasielastic neutron scattering measurements on $HfTi_2H_4$, $HfTi_2H_{3.5}$ and $ZrTi_2H_{3.9}$ have confirmed the existence of a fast localized H motion in these hydrogen-stabilized phases. The behaviour of the elastic incoherent structure factor is consistent with H jumps within the hexagons formed by interstitial g sites. The fraction of H atoms participating in the fast localized motion increases with increasing temperature. Our results support the following microscopic picture of H diffusion in C15-type $HfTi_2H_x$ and $ZrTi_2H_x$ phases. Most of the H atoms occupy the nearly completely filled sublattice of e sites. In order to move from one e site to another, a hydrogen atom has to jump to the nearest g site. The g-site sublattice is characterized by the short nearest-neighbour g–g distances and by the low degree of H filling. Therefore, a hydrogen atom can easily move on the g-site sublattice, and, in particular, it can participate in the fast localized motion over g-site hexagons. Each H atom jumping out of the

e-site sublattice is expected to perform a number of jumps on the g-sublattice before it finds a vacant e site. A similar mechanism of H diffusion has been reported for the ordered β-V_2H phase [18], where the filled (110) planes of octahedral interstitial sites are separated by the empty (110) planes. The parameters of H motion in the hydrogen-stabilized phases $HfTi_2H_x$ and $ZrTi_2H_x$ with $x \approx 4$ are found to be close to each other. The characteristic hopping rate τ_l^{-1} of the localized H motion in $HfTi_2H_4$ is somewhat higher than in $ZrTi_2H_{3.9}$. This is consistent with the shorter nearest-neighbour g–g distance r_{g1} for $HfTi_2H_4$. On the other hand, the long-range diffusivity of hydrogen at room temperature in $HfTi_2H_4$ appears to be somewhat lower than in $ZrTi_2H_{3.9}$.

Acknowledgments

References

[1] Miron N F, Shcherbak V I, Bykov V N and Levdik V A 1971 *Sov. Phys.–Crystallogr.* **16** 266
[2] Kozhanov V N, Skripov A V and Romanov E P 1998 *J. Alloys Compounds* **269** 141
[3] Somenkov V A and Irodova A V 1984 *J. Less-Common Met.* **101** 481
[4] Yvon K and Fischer P 1988 *Hydrogen in Intermetallic Compounds I* ed L Schlapbach (Berlin: Springer) p 87
[5] Fischer P, Fauth F, Böttger G, Skripov A V and Kozhanov A P 1999 *J. Alloys Compounds* **282** 184
[6] Skripov A V, Cook J C, Sibirtsev D S, Karmonik C and Hempelmann R 1998 *J. Phys.: Condens. Matter* **10** 1787
[7] Skripov A V, Pionke M, Randl O and Hempelmann R 1999 *J. Phys.: Condens. Matter* **11** 1489
[8] Skripov A V, Cook J C, Karmonik C and Kozhanov V N 1999 *Phys. Rev.* B **60** 7238
[9] Skripov A V, Rychkova S V, Belyaev M Yu and Stepanov A P 1989 *Solid State Commun.* **71** 1119
[10] Renz W, Majer G and Skripov A V 1995 *J. Alloys Compounds* **224** 127
[11] Fernandez J F, Kemali M, Johnson M R and Ross D K 1997 *Physica* B **234–236** 903
[12] Bée M 1988 *Quasielastic Neutron Scattering* (Bristol: Hilger)
[13] Chudley C T and Elliott R J 1961 *Proc. Phys. Soc.* **77** 353
[14] Yvon K 1984 *J. Less-Common Met.* **103** 53
[15] Skripov A V, Sibirtsev D S and Kozhanov V N 2000 to be published
[16] Kozhanov V N, Skripov A V, Stepanov A P, Romanov E P and Buzlukov A L 1999 *Fiz. Met. Metalloved.* **88** 58 (Engl. Transl. 1999 *Phys. Met. Metallogr.* **88** 58)
[17] Schönfeld C, Hempelmann R, Richter D, Springer T, Dianoux A J, Rush J J, Udovic T J and Bennington S M 1994 *Phys. Rev.* B **50** 853
[18] Richter D, Mahling-Ennaoui S and Hempelmann R 1989 *Z. Phys. Chem., NF* **164** 907
[19] Tahir-Kheli R A and Elliott R J 1983 *Phys. Rev.* B **27** 844